THIRD EDITION

Tunable Laser Applications

EDITED BY F.J. DUARTE

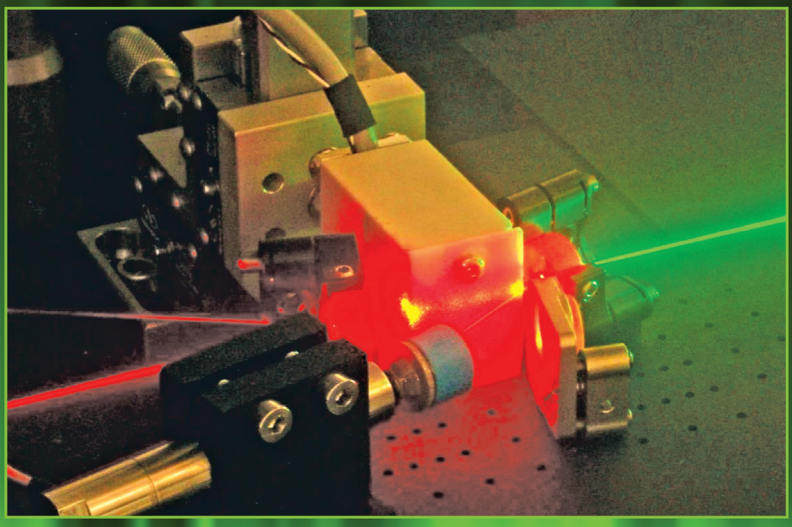

CRC Press
Taylor & Francis Group

THIRD EDITION

Tunable Laser Applications

OPTICAL SCIENCE AND ENGINEERING

Founding Editor
Brian J. Thompson
University of Rochester
Rochester, New York

RECENTLY PUBLISHED

Tunable Laser Applications, Third Edition, *edited by F. J. Duarte*
Laser Safety: Tools and Training, Second Edition, *edited by Ken Barat*
Optical Materials and Applications, *edited by Moriaki Wakaki*
Lightwave Engineering, *Yasuo Kokubun*
Handbook of Optical and Laser Scanning, Second Edition, *Gerald F. Marshall and Glenn E. Stutz*
Computational Methods for Electromagnetic and Optical Systems, Second Edition, *John M. Jarem and Partha P. Banerjee*
Optical Methods of Measurement: Wholefield Techniques, Second Edition, *Rajpal S. Sirohi*
Optoelectronics: Infrared-Visible-Ultraviolet Devices and Applications, Second Edition, *edited by Dave Birtalan and William Nunley*
Photoacoustic Imaging and Spectroscopy, *edited by Lihong V. Wang*
Polarimetric Radar Imaging: From Basics to Applications, *Jong-Sen Lee and Eric Pottier*
Near-Earth Laser Communications, *edited by Hamid Hemmati*
Slow Light: Science and Applications, *edited by Jacob B. Khurgin and Rodney S. Tucker*
Dynamic Laser Speckle and Applications, *edited by Hector J. Rabal and Roberto A. Braga Jr.*
Biochemical Applications of Nonlinear Optical Spectroscopy, *edited by Vladislav Yakovlev*
Optical and Photonic MEMS Devices: Design, Fabrication and Control, *edited by Ai-Qun Liu*
The Nature of Light: What Is a Photon?, *edited by Chandrasekhar Roychoudhuri, A. F. Kracklauer, and Katherine Creath*
Introduction to Nonimaging Optics, *Julio Chaves*
Introduction to Organic Electronic and Optoelectronic Materials and Devices, *edited by Sam-Shajing Sun and Larry R. Dalton*
Fiber Optic Sensors, Second Edition, *edited by Shizhuo Yin, Paul B. Ruffin, and Francis T. S. Yu*
Terahertz Spectroscopy: Principles and Applications, *edited by Susan L. Dexheimer*
Photonic Signal Processing: Techniques and Applications, *Le Nguyen Binh*
Smart CMOS Image Sensors and Applications, *Jun Ohta*
Organic Field-Effect Transistors, *Zhenan Bao and Jason Locklin*
Coarse Wavelength Division Multiplexing: Technologies and Applications, *edited by Hans Joerg Thiele and Marcus Nebeling*

Please visit our website ***www.crcpress.com*** *for a full list of titles*

THIRD EDITION

Tunable Laser Applications

EDITED BY

F.J. DUARTE

Interferometric Optics

Rochester, New York, USA

CRC Press

Taylor & Francis Group

Boca Raton London New York

CRC Press is an imprint of the
Taylor & Francis Group, an **informa** business

CRC Press
Taylor & Francis Group
6000 Broken Sound Parkway NW, Suite 300
Boca Raton, FL 33487-2742

Version Date: 20151112

International Standard Book Number-13: 978-1-4822-6107-3 (eBook - PDF)

Dedication

In memory of our dear friends, colleagues, and coauthors:
Roberto Sastre (1944–2010) and Robert Owens James (1944–2015).

This page intentionally left blank

Contents

Preface

Broadly tunable lasers continue to have a tremendous impact in many and diverse fields of science and technology. From a renaissance in laser spectroscopy, to Bose–Einstein condensation, the one nexus is … *the tunable laser.* In this regard, numerous applications, from physics, to isotope separation, and all the way to medicine, depend on the tunable laser. This third edition includes 14 chapters. In this collection of chapters, two chapters are new, and all the other chapters have been updated and extended in their coverage. The subject matter ranges from the physics of tunable coherent sources and coherent microscopic instrumentation to exciting applications such as astronomy, defense, medicine, laser isotope separation, microscopy, and spectroscopy.

It is indeed a pleasure to offer to the scientific community this updated and enlarged third edition of *Tunable Laser Applications.* As editor, I remain indebted to all the contributing authors.

F. J. Duarte
Rochester, New York

This page intentionally left blank

Editor

F. J. Duarte is a research physicist with Interferometric Optics, Rochester, New York, and adjunct professor at Electrical and Computer Engineering, University of New Mexico. He graduated with first-class honors in physics from the School of Mathematics and Physics at Macquarie University (Sydney, Australia), where he was also awarded a PhD in physics for his research on optically pumped molecular lasers. At Macquarie, he was a student of the well-known quantum physicist J. C. Ward. Duarte's research has taken place at a number of institutions in academia, industry, and the defense establishment. Dr. Duarte is the author of the generalized multiple-prism dispersion theory and has made various unique contributions to the physics and architecture of tunable laser oscillators. He has also pioneered the use of Dirac's quantum notation in interferometry, oscillator physics, and classical optics. These contributions have found applications in the design of laser resonators, laser pulse compression, imaging, microscopy, medicine, optics communications, the nuclear industry, and quantum entanglement. He is the lead author of numerous refereed papers and several U.S. patents. Dr. Duarte is author and editor of *Dye Laser Principles* (Academic 1990), *High-Power Dye Lasers* (Springer 1991), *Selected Papers on Dye Lasers* (SPIE 1992), *Tunable Lasers Handbook* (Academic 1995), *Tunable Laser Applications* (1st edn, Marcel Dekker 1995; 2nd edn, CRC Press 2009; 3rd edn, CRC Press 2016), *Coherence and Ultrashort Pulsed Laser Emission* (InTech 2010), and *Laser Pulse Phenomena and Applications* (InTech 2010). He is also the sole author of *Tunable Laser Optics* (1st edn, Elsevier-Academic 2003; 2nd edn, CRC Press 2015) and *Quantum Optics for Engineers* (CRC Press 2014). Dr. Duarte is a fellow of the Australian Institute of Physics and a fellow of the Optical Society, and received the Engineering Excellence Award from the Optical Society of America.

This page intentionally left blank

Contributors

A. Costela
Instituto de Química Física
"Rocasolano", C.S.I.C.
Madrid, Spain

F. J. Duarte
Interferometric Optics
Rochester, New York

and

Electrical and Computer Engineering
University of New Mexico
Albuquerque, New Mexico

I. García-Moreno
Instituto de Química Física
"Rocasolano", C.S.I.C.
Madrid, Spain

C. Gómez
Instituto de Química Física
"Rocasolano", C.S.I.C.
Madrid, Spain

J. G. Haub
Laser Technologies Group
Cyber & Electronic Warfare Division
Defence Science and Technology Group
Edinburgh, South Australia, Australia

Y. He
National Measurement Institute

and

MQ Photonics Research Centre
Department of Physics and Astronomy
Macquarie University
Sydney, New South Wales, Australia

R. O. James
Interferometric Optics
Rochester, New York

B. J. Orr
MQ Photonics Research Centre
Department of Physics and Astronomy
Macquarie University
Sydney, New South Wales, Australia

S. Popov
Royal Institute of Technology
Stockholm, Sweden

R. Sastre
Instituto de Ciencia y Tecnología de Polímeros, C.S.I.C.
Madrid, Spain

T. M. Shay
Shay Electro-Optical Engineering
Saint George, Utah

R. T. White
Institute for Photonics and Advanced Sensing and School of Physical Sciences
The University of Adelaide
Adelaide, South Australia, Australia

This page intentionally left blank

1 Introduction

F. J. Duarte

CONTENTS

1.1 INTRODUCTION

The ability to yield tunable coherent radiation enhances the applicability of a given laser substantially. Indeed, tunable lasers are among the most studied and successful lasers known today. For instance, the first broadly tunable laser, *the organic dye laser*, introduced circa 1966 [1–4], has enjoyed a significant amount of attention directed toward the study of its inherent physical properties and technology [5–12]. At the same time, these organic lasers have had a profound impact on a plethora of fields, including physics, spectroscopy, laser isotope separation, medicine, and astronomy [6,13–16].

Today, the field of broadly tunable lasers includes an array of different lasers, which have markedly extended the applicability domain of lasers. In addition to the broadly tunable organic dye lasers, there are broadly tunable semiconductor lasers, optical parametric oscillators (OPOs), tunable fiber lasers, tunable quantum cascade lasers, and free electron lasers (FELs). Also, at this stage, it should be realized that in addition to the class of broadly tunable lasers, there is an additional group of discretely tunable or line-tunable lasers. This latter class of laser, besides being able to shift emission frequency from transition to transition, can also be fine-tuned within the emission spectrum of a given transition.

In Tables 1.1 through 1.5, basic tuning ranges and energetic properties of tunable sources of coherent radiation are provided to facilitate rapid familiarity with the emission characteristics offered by these sources.

Table 1.1 lists the wavelength coverage published for various broadly tunable pulsed sources of coherent radiation, including the OPO and the FEL. Table 1.2 lists reported short pulse durations demonstrated in several types of broadly tunable lasers, while Table 1.3 includes the energetic and power characteristics capabilities for tunable pulsed lasers.

Table 1.4 lists the emission characteristics from broadly tunable lasers in the continuous-wave (CW) regime, including wavelength range and reported

TABLE 1.1
Wavelength Range of Broadly Tunable Coherent Sources in the Pulsed Regime

Tunable Source	Spectral Range
Dye laser	$320 \leq \lambda \leq 1200$ nm[a] [17]
$Ti^{3+}:Al_2O_3$ laser	$660 \leq \lambda \leq 986$ nm [18]
$Cr^{3+}:BeAl_2O_4$ laser	$701 \leq \lambda \leq 818$ nm [19]
Fiber laser[b]	$980 \leq \lambda \leq 1070$ nm [20]
OPO (BBO)[c]	$0.3 \leq \lambda \leq 3.0$ μm [21]
OPO (KTP)[c]	$0.7 \leq \lambda \leq 4.0$ μm [21]
FEL	$0.9 \leq \lambda \leq 10$ μm[d] [22]
	$830 \leq \lambda \leq 940$ nm[e] [23]
	$31 \leq \lambda \leq 32$ nm [24]

[a] Tuning range resulting from the use of several dyes.
[b] Yb-doped fiber.
[c] BBO, β-barium borate; KTP, potassium titanyl phosphate.
[d] The combined tuning range from various FEL facilities extends into the millimeter range.
[e] Large bandwidth.

TABLE 1.2
Short Pulse Emission Characteristics of Broadly Tunable Coherent Sources

Tunable Source	Δt
Dye laser	6 fs[a] [25]
$Ti^{3+}:Al_2O_3$ laser	5 fs[b] [26]
ECS[c] laser (AlGaAs)	200 fs[a] [27]
Fiber laser	24 fs [28]
OPO (BBO)	4 fs [29]
FEL	25 fs [30]

[a] Using prismatic intracavity pulse compression.
[b] Using extracavity in addition to intracavity pulse compression.
[c] Semiconductor.

laser power. It should be noted that although some types of lasers have been reported with higher power figures at a single emission wavelength, these are not included, given the emphasis on broad wavelength tunability. The extension of the tuning ranges cited in these tables can be established via nonlinear optical techniques [6,11].

TABLE 1.3
Energetic Characteristics of Broadly Tunable Coherent Sources in the Pulsed Regime[a]

Tunable Source	Pulse Energy	Average Power
Dye laser	400 J[b] [31]	2.5 kW[c] [16]
$Ti^{3+}:Al_2O_3$ laser	6.5 J[d] [32]	5.5 W[e] [33]
$Cr^{3+}:BeAl_2O_4$ laser	100 J[f] [34]	—
Fiber laser[f]	31 nJ [35]	3 W [35]
OPO (BBO)	>100 mJ [36]	5.4 W [37]
FEL	—	100 W[g] [22]

[a] Energy and average power figures are from unrelated experiments.
[b] From a flashlamp-pumped dye laser.
[c] CVL-pumped dye laser operating at a prf of 13.2 kHz.
[d] Under flashlamp excitation.
[e] Under CVL excitation at a prf of 6.5 kHz.
[f] Oscillator amplifier configuration using a Tm-doped amplifier. System is tunable in the 1900–2040 nm region [35].
[g] Under broadly tunable conditions at the FEL of the Thomas Jefferson National Accelerator Facility. The average power can increase to over 10 kW at selected individual wavelengths [22].

Spectral information on discretely tunable pulsed lasers is given in Table 1.5; line-tunable CW lasers such as Ar^+, Kr^+, He–Ne, and He–Cd are listed in Table 10.1 (Chapter 10). An interesting laser listed in Table 1.5 is XeF. It can be classified as discretely tunable, given the characteristics of its $B \rightarrow X$ transitions. However, the wide tunability of its $C \rightarrow A$ transition qualifies it as a broadly tunable laser. At this stage, it should be mentioned that a distinct feature of the gas lasers listed in Table 1.5 is their ability to yield high pulse energies and, in some cases, very high average powers [16].

1.2 TUNABLE LASER COMPLEMENTARITY

The information conveyed in Tables 1.1 through 1.5 suggests that the field offers a wide variety of sources of tunable coherent radiation that have distinct optimal modes of operation. Hence, a useful generalized approach to the field should be from a perspective of complementarity. This principle of *tunable laser complementarity* [64,65] offers a dual advantage, which encourages the use of the most efficient and apt type of laser for a given application, and the integration of different lasers into a single system if necessary. This latter approach has been fairly well demonstrated in hybrid laser systems using one class of laser at the oscillator stage and a different type of laser at the amplifier stage. Examples of these systems involve the use of a dye laser oscillator and an XeF laser amplifier [54], a semiconductor laser oscillator

TABLE 1.4
Emission Characteristics Available from Broadly Tunable Sources of Coherent Radiation in the CW Regime

Tunable Source	Spectral Range	CW Power
Dye laser	$365 \leq \lambda \leq 1000$ nm[a] [38]	43 W[b] [39]
$Ti^{3+}:Al_2O_3$ laser	$710 \leq \lambda \leq 870$ nm[c] [40]	43 W[b,d] [41]
$Cr^{3+}:BeAl_2O_4$ laser	$744 \leq \lambda \leq 788$ nm	6.5 W [42]
ECS laser (InGaAsP/InP)	$1255 \leq \lambda \leq 1335$ nm[e]	≥1 mW [43]
ECS laser (GaAlAs)	$815 \leq \lambda \leq 825$ nm	5 mW [44]
ECS laser array	$750 \leq \lambda \leq 758$ nm	13.5 W [45]
EC QCL[f]	$8.2 \leq \lambda \leq 10.4$ μm	15 mW [46]
EC QCL[f]	$7.6 \leq \lambda \leq 11.4$ μm[g]	65 μW [47]
OPO (PPLN[j])	$3.3 \leq \lambda \leq 3.9$ μm	>1 W [48]
Fiber laser	$1032 \leq \lambda \leq 1124$ nm[h]	10 W [49]
Fiber laser	$1532 \leq \lambda \leq 1568$ nm[i]	>100 W [50]

[a] Tuning range resulting from the use of several dyes.
[b] Under Ar^+ laser excitation.
[c] Tuning range of single-longitudinal-mode emission.
[d] Uses liquid-nitrogen cooling.
[e] Measured laser linewidth is $\Delta\nu \leq 100$ kHz [43].
[f] QCL, quantum cascade laser.
[g] Measured laser linewidth is $\Delta\nu \approx 2.5$ GHz [47].
[h] Measured laser linewidth is $\Delta\nu \approx 3.6$ GHz [49].
[i] Measured laser linewidth is $\lambda \approx 1$ nm [50].
[j] PPLN, periodically poled lithium niobate.

in conjunction with a dye laser amplifier [66], and a solid-state dye laser oscillator [67] with an OPO as amplifier [68]. A better-known example of complementarity is the excitation of one class of laser by a different type of laser. Recent versions of this synergy include the fiber laser excitation of an optical parametric amplifier (OPA) [69] and the fiber laser excitation of tunable mid-infrared (IR) solid-state lasers [70]. Albeit arguably more attractive examples than those listed might be available, the principal message is that different types of lasers can be integrated in a system to provide an optimum solution.

However, more fundamental than the skillful integration of hybrid systems is the appropriate, and most efficient, use of a laser system for a given application. For instance, if an application requires high average powers, in the $580 \leq \lambda \leq 590$ nm region, the choice should still be a copper-vapor laser (CVL)–pumped dye laser. If large pulsed energies, tens or hundreds of joules per pulse, were necessary in the same spectral region, then a flashlamp-pumped dye laser would have to be considered. On the other hand, for an application requiring very narrow-linewidth CW emission in the near IR, an external-cavity semiconductor (ECS) laser should be the preference. Further, for spectroscopic applications demanding considerable

TABLE 1.5
Spectral Emission Characteristics of Discretely Tunable High-Power Pulsed Lasers

Laser	Transition	Bandwidth (GHz)	Wavelength (nm)
ArF	—	~17,000[a] [51]	193
KrF	$B^2\Sigma^+_{1/2} - X^2\Sigma^+_{1/2}$	~10,500[a] [51]	248
XeCl	$B^2\Sigma^+_{1/2} - X^2\Sigma^+_{1/2}$	374 [52]	308
	—	397 [52]	308.2
XeF	*B–X*	187 [53]	351
	—	330 [53]	353
	C–A	—	466–514[a] [54]
N_2	$C^3\Pi_u$–$B^3\Pi_g$	203 [55]	337.1
HgBr	—	918 [56]	502
	—	1,012 [56]	504
Ca^{2+}	$5^2S_{1/2}$–$4^2P_{3/2}$	—	373.7
Sr^{2+}	$6^2S_{1/2}$–$5^2P_{3/2}$	2–12[b] [57]	430.5
Cd^{2+}	$4^2F_{5/2}$–$5^2D_{3/2}$	—	533.7
Cu	$^2P_{3/2}$–$^2D_{5/2}$	7 [58]	510.5
	$^2P_{1/2}$–$^2D_{3/2}$	11 [58]	578.2
Au	$^2P_{1/2}$–$^2D_{3/2}$	1.5 [59]	627.8
Nd:YAG	$^4F_{3/2}$–$^4I_{11/2}$	15–32	1,064
CO_2	P14(00°1–10°0)[c]	—	10,532.09
	P16(00°1–10°0)	—	10,551.40
	P18(00°1–10°0)	—	10,571.05
	P20(00°1–10°0)	3–4[d] [60]	10,591.04

[a] Tuning range.
[b] Variable-linewidth range.
[c] Emission transitions obtained in a hybrid CO_2 laser [61]. For a comprehensive listing of CO_2 laser transitions, see [62].
[d] Observed bandwidth in a transversely excited atmospheric pressure CO_2 laser in the absence of intracavity linewidth-narrowing optics or injection from a CW CO_2 laser. Tunable narrow-linewidth emission, at $\Delta\nu \approx 107$ MHz, has been reported for this transition [63].

wavelength agility throughout the visible, an OPO system would be a most attractive option. In this context, at present, tunable fiber lasers appear best suited for applications requiring high-CW powers in the near IR. This perspective of complementarity is compatible with the rationale that, under ideal conditions, *it should be the application that determines the use of a particular laser* [71,72]. Note that under this utilitarian rationale, complementarity does not marginalize competition.

The logic to determine the usefulness of a given laser for an application of interest should follow the criteria of providing tunable coherent radiation, at a given spectral region, within specified emission parameters, using the simplest and most efficient means. However, in practice, this approach can be complicated by extraneous issues, such as existing managerial guidelines or cost constraints.

In the absence of extraneous constraints, parameters that should determine the suitability of a laser to a given application include the required spectral region of emission, tuning range, output power or energy, emission linewidth, and amplified spontaneous emission (ASE) level. In the case of pulsed lasers, pulse duration and pulse repetition frequency (prf) can often be considered important parameters.

At this juncture, it should be mentioned that although the word *laser* has been used throughout this chapter, an important source of coherent tunable radiation, the OPO, does not involve the process of population inversion. Nevertheless, what is important is that this source emits tunable coherent radiation that is indistinguishable from laser radiation. Hence, the title of the book and the ample use of the word laser are justified.

1.3 TUNABLE LASER APPLICATIONS

Applications for tunable lasers are extraordinarily widespread and varied, so that only some limited highlights can be mentioned in this introduction. For instance, the dye laser alone has been applied to physics [73–75], astronomy [16], spectroscopy [15,76–79], laser isotope separation [16,80–95], material diagnostics [96], material processing [96,97], remote sensing [96,98,99], defense [17,87,100], and medicine [101].

Tunable solid-state coherent sources have found numerous applications, including spectroscopy [21,102,103], and remote sensing [104]. A remarkable application of short-pulse solid-state lasers has been their use in the generation of frequency combs for *optical clockworks* [105,106], which has led to a revolution in high-precision optical measurements.

Tunable semiconductor lasers are particularly well suited for application to atomic physics [107–109] and spectroscopy [110,111]. These sources are also useful in application to metrology, interferometry, and imaging. Furthermore, simple and compact external-cavity tunable semiconductor lasers have made essential contributions to studies in laser cooling [108,110] and Bose–Einstein condensation [112]. They have also been applied to laser isotope separation [113] and have become a central component in the field of optical communications [114].

1.4 TUNABLE LASER APPLICATIONS: 1ST EDITION

The first edition of *Tunable Laser Applications* [115], published in 1995, included the following chapters:

1. Introduction, by F. J. Duarte
2. Spectroscopic Applications of Pulsed Tunable Optical Parametric Oscillators, by B. J. Orr, M. J. Johnson, and J. G. Haub
3. Dispersive External Cavity Semiconductor Lasers, by F. J. Duarte

4. Applications of Ultrashort Pulses, by X. M. Zhao, S. Diddams, and J. C. Diels
5. Interferometric Imaging, by F. J. Duarte
6. Medical Applications of the Free Electron Laser, by F. E. Carroll and C. A. Brau
7. Lidar for Atmospheric and Hydrospheric Studies, by W. B. Grant

1.5 TUNABLE LASER APPLICATIONS: 2ND EDITION

The second edition of *Tunable Laser Applications* [116], published in 2009, included the following chapters:

1. Introduction, by F. J. Duarte
2. Spectroscopic Applications of Tunable Optical Parametric Oscillators, by B. J. Orr, Y. He, and R. T. White
3. Solid State Dye Lasers, by A. Costela, I. García-Moreno, and R. Sastre
4. Tunable Lasers Based on Dye-Doped Polymer Gain Media Incorporating Homogeneous Distributions of Functional Nanoparticles, by F. J. Duarte and R. O. James
5. Broadly Tunable External-Cavity Semiconductor Lasers, by F. J. Duarte
6. Tunable Fiber Lasers, by T. M. Shay and F. J. Duarte
7. Fiber Laser Overview and Medical Applications, by S. Popov
8. Medical Applications of Dye Lasers, by A. Costela, I. García-Moreno, and R. Sastre
9. Biological Microscopy with Ultrashort Laser Pulses, by J. L. Thomas and W. Rudolph
10. Pulsed, Tunable, Monochromatic X-Rays: Medical and Nonmedical Applications, by F. E. Carroll
11. Lithium Spectroscopy Using Tunable Diode Lasers, by I. E. Olivares
12. Interferometric Imaging, by F. J. Duarte
13. Multiple-Prism Arrays and Multiple-Prism Beam Expanders: Laser Optics and Scientific Applications, by F. J. Duarte
14. Coherent Electrically Excited Organic Semiconductors, by F. J. Duarte
15. Appendix on Optical Quantities and Conversion Units, by F. J. Duarte

In fairness to readers, in this new edition, it was decided not to reproduce a chapter unless it had been updated by at least one of the original authors. Thus, Chapters 1 through 8 and Chapters 12 through 15 are included in this third edition of *Tunable Laser Applications* [117] in an expanded and updated format. In addition, two new chapters extend the scope and coverage of this third edition, which is introduced and explained in the next section.

1.6 FOCUS OF THIS BOOK

The purpose of this book is to focus on topics that highlight the utilitarian ethos of tunable lasers. In this regard, the emphasis in this book is to highlight the synergy

between tunable laser development and *tunable laser applications*. The topics selected focus on applications judged to be of broad interest, historical significance, and sustained value: spectroscopy, laser isotope separation, selective laser excitation, biology, medicine, imaging, and interferometry. Among these, one of the most prevalent themes of interest in this third edition of *Tunable Laser Applications* continues to be medicine and biomedical applications.

Although there is no predetermined order of presentation, and each chapter can be read independently, Chapters 2 through 5 deal with issues of gain media, device physics, and technology. Chapter 2, written by B. J. Orr, J. G. Haub, Y. He, and R. T. White, is entitled "Spectroscopic Applications of Pulsed Tunable Optical Parametric Oscillators" and is the leading chapter, given the wider spectral coverage of these sources of coherent radiation and its extensive and detailed discussion on spectroscopy. In this new edition, this chapter has been substantially updated and enlarged, thus providing perhaps the most complete and authoritative treatise on the application of optical parametric oscillators available in the contemporary literature. The applications sections include biomedical, defense, and microscopy applications.

Chapter 3, authored by A. Costela, I. García-Moreno, and R. Sastre, is entitled "Solid-State Organic Dye Lasers," and focuses on solid-state dye lasers, with a thorough emphasis on organic and organic–inorganic gain media. Chapter 4, by F. J. Duarte and R. O. James, entitled "Organic Dye-Doped Polymer-Nanoparticle Tunable Lasers," provides an updated performance survey of tunable narrow-linewidth solid-state dye lasers and describes the characteristics of new dye-doped polymer gain media incorporating homogeneous nanoparticle distributions. Chapter 5, by F. J. Duarte, entitled "Broadly Tunable Dispersive External-Cavity Semiconductor Lasers," focuses on the performance of dispersive external-cavity semiconductor lasers and describes intracavity optics and tuning methods that are also relevant to other tunable sources of coherent radiation discussed in this book. Both Chapters 4 and 5 include a brief survey of biomedical applications. Chapter 6, written by T. M. Shay and F. J. Duarte, is entitled "Tunable Fiber Lasers" and focuses on the main approaches currently used to achieve tunability in these lasers. This is followed by Chapter 7, by S. Y. Popov, which is entitled "Fiber Laser Overview and Medical Applications." This chapter provides a survey of fiber laser gain media and introduces the reader to the medical applications of these lasers. This chapter signals a shift in emphasis in the book toward applications.

The emphasis on medical and biomedical applications becomes a central theme in Chapter 8. This chapter is authored by A. Costela, I. García-Moreno, and C. Gómez and is entitled "Medical Applications of Organic Dye Lasers." This work provides an updated and extensive survey of the applications of tunable dye lasers to medicine, including subjects such as dermatology, photodynamic therapy, and lithotripsy. Chapter 9, written by F. J. Duarte, is entitled "Tunable Laser Microscopy" and provides a survey of various coherent techniques used in the fields of microscopy and nanoscopy. Biomedical applications are also considered in Chapter 10, written by F. J. Duarte, which is on "Interferometric Imaging." This chapter also considers applications of *N*-slit interferometric techniques in optical metrology and optical free-space communications.

The following chapter focuses on selective laser excitation. Chapter 11, by F. J. Duarte, is entitled "Tunable Laser Atomic Vapor Laser Isotope Separation" and provides an overview of this field, mainly from the perspective of high-power tunable lasers.

The remaining two chapters focus on multiple-prism optics and its applications, plus coherent emission from organic semiconductors. Chapter 12, by F. J. Duarte, focuses on a description of experiments on electrically excited pulsed organic semiconductors and is entitled "Coherent Electrically Excited Organic Semiconductors." Chapter 13, by F. J. Duarte, is entitled "Multiple-Prism Arrays and Multiple-Prism Beam Expanders: Laser Optics and Scientific Applications," and provides a brief referenced survey of numerous fields of applications that use multiple-prism arrays either directly, deployed within a narrow-linewidth tunable laser, or deployed within an ultrashort pulse laser. The book concludes with Chapter 14, by F. J. Duarte, listing useful optical quantities and explaining the linewidth equivalence, which is entitled "Optical Quantities and Conversion Units."

Tunable Laser Applications includes the applications of tunable coherent sources, in various degrees of detail, to the following fields:

Astronomy
Atomic spectroscopy
Biomedicine
Coherent Raman microscopy
Communications
Characterization of textiles
Defense
Densitometry
Dentistry
Dermatology
Digital imaging
Digital microscopy
Environmental monitoring
Infrared countermeasures
Interferometric communications
Interferometric imaging
Interferometric microscopy
Interferometry
Laser cooling
Laser guide star
Laser isotope separation
Laser printing
Laser pulse compression
Light sheet microscopy
Medical applications of dye lasers
Medical applications of fiber lasers
Microdensitometry
Molecular spectroscopy

Nanoparticle transparency
Optical coherence tomography (OCT)
Optical metrology
Photodynamic therapy
Surgery
Ultrashort pulse microscopy

ACKNOWLEDGMENTS

This third edition of *Tunable Laser Applications* has been made possible by the support of Interferometric Optics and the integrated effort of the contributing authors. In addition to discussions of laser physics and technology, they have provided an up-to-date and vibrant description of an enormous variety of applications of tunable sources of coherent radiation. The encouragement and cooperation of Ashley Gasque at CRC Press is also acknowledged.

REFERENCES

1. Sorokin, P. P. and J. R. Lankard, Stimulated emission observed from an organic dye, chloroaluminum phthalocyanine, *IBM J. Res. Dev.* 10: 162–163, 1966.
2. Schäfer, F. P., W. Schmidt, and J. Volze, Organic dye solution laser, *Appl. Phys. Lett.* 9: 306–309, 1966.
3. Soffer, B. H. and B. B. McFarland, Continuously tunable narrow-band organic dye lasers, *Appl. Phys. Lett.* 10: 266–267, 1967.
4. Stepanov, B. I., A. N. Rubinov, and V. A. Mostovnikov, Optic generation in solutions of complex molecules, *JETP Lett.* 5: 117–119, 1967.
5. Schäfer, F. P. (Ed.), *Dye Lasers*, Springer, Berlin, 1990.
6. Duarte, F. J. and L. W. Hillman (Eds), *Dye Laser Principles*, Academic, New York, 1990.
7. Duarte, F. J. (Ed.), *High Power Dye Lasers*, Springer, Berlin, 1991.
8. Stuke, M. (Ed.), *Dye Lasers: 25 Years*, Springer, Berlin, 1992.
9. Duarte, F. J. (Ed.), *Selected Papers on Dye Lasers*, SPIE Optical Engineering, Bellingham, WA, 1992.
10. Duarte, F. J. (Ed.), *Tunable Lasers Handbook*, Academic, New York, 1995.
11. Duarte, F. J., *Tunable Laser Optics*, Academic, New York, 2003.
12. Maeda, M., *Laser Dyes*, Academic, New York, 1984.
13. Radziemski, L. J., R. W. Solarz, and J. A. Paisner (Eds), *Laser Spectroscopy and Its Applications*, Marcel Dekker, New York, 1987.
14. Duarte, F. J., J. A. Paisner, and A. Penzkofer, Dye lasers: Introduction by the feature editors, *Appl. Opt.* 31: 6977–6878, 1992.
15. Demtröder, W., *Laser Spectroscopy*, 3rd edn, Springer, Berlin, 2003.
16. Bass, I. L., R. E. Bonanno, R. P. Hackel, and P. R. Hammond, High-average-power dye laser at Lawrence Livermore National Laboratory, *Appl. Opt.* 31: 6993–7006, 1992.
17. Duarte, F. J. and L. W. Hillman, Introduction. In F. J. Duarte and L. W. Hillman (Eds), *Dye Laser Principles*, Chapter 1, Academic, New York, 1990.
18. Moulton, P. F., Spectroscopic and laser characteristics of Ti:Al_2O_3, *J. Opt. Soc. Am. B* 3: 125–132, 1986.
19. Walling, J. C., O. G. Peterson, H. P. Jenssen, R. C. Morris, and E. W. O'Dell, Tunable alexandrite lasers, *IEEE J. Quantum Elect.* QE–16: 1302–1315, 1980.

20. Okhonikov, O. G., L. Gomes, N. Xiang, T. Jouhti, and A. B. Grudinin, Mode-locked ytterbium fiber laser tunable in the 980–1070 nm spectral range, *Opt. Lett.* 28: 1522–1524, 2003.
21. Orr, B. J., M. J. Johnson, and J. B. Haub, Spectroscopic applications of pulsed tunable optical parametric oscillators. In F. J. Duarte (Ed.), *Tunable Laser Applications*, 1st edn, Chapter 2, Marcel-Dekker, New York, 1995.
22. Benson, S. V., Private communication, 2007.
23. Andonian, G., A. Murokh, J. B. Rosenzweig, R. Agustsson, M. Babzien, I. Ben-Zvi, P. Frigola, et al., Observations of anomalously large spectral bandwidth in a high-gain self- amplified spontaneous emission free electron laser, *Phys. Rev. Lett.* 95: 054801, 2005.
24. Düsterer, S., P. Radcliffe, G. Geloni, U. Jastrow, M. Kuhlmann, E. Plönjes, K. Tiedke, P., et al., Spectroscopic characterization of vacuum ultraviolet free electron laser pulses, *Opt Lett.* 31: 1150–1152, 2006.
25. Fork, R. L., C. H. Brito-Cruz, P. C. Becker, and C. V. Shank, Compression of optical pulses to six femtoseconds by using cubic phase compensation, *Opt. Lett.* 12: 483–485, 1987.
26. Ell, R., U. Morgner, F. X. Kärtner, J. G. Fujimoto, E. P. Ippen, V. Scheuer, G. Angelow, et al., Generation of 5-fs pulses and octave-spanning spectra directly from a Ti:sapphire laser, *Opt. Lett.* 26: 373–375, 2001.
27. Delfyett, P. J., L. Florez, N. Stoffel, T. Gmitter, N. Andreadakis, G. Alphonse, and W. Ceislik, 200 fs optical pulse generation and intracavity pulse evolution in a hybrid mode-locked semiconductor diode-laser/amplifier system, *Opt. Lett.* 17: 670–672, 1992.
28. Tauser, F., F. Adler, and A. Leitenstorfer, Widely tunable sub-30-fs pulses from a compact erbium-doped fiber source, *Opt. Lett.* 29: 516–518, 2004.
29. Baltuska, A., T. Fuji, and T. Kobayashi, Visible pulse compression to 4 fs by optical parametric amplification and programmable dispersion control, *Opt. Lett.* 27: 306–308, 2002.
30. Chalupsky, J., L. Juha, J. Kuba, J. Cihelka, V. Hájková, S. Koptyaev, J. Krása, et al., Characteristics of focused soft X-ray free-electron laser beam determined by ablation of organic molecular solids, *Opt. Express* 15: 6036–6043, 2007.
31. Baltakov, F. N., B. A. Garikhin, and L. V. Sukhanov, 400-J pulsed laser using a solution of rhodamine 6 G in ethanol, *JETP Lett.* 19: 174–175, 1974.
32. Brown, A. J. W. and C. H. Fisher, A 6.5-J flashlamp-pumped Ti:Al_2O_3 laser, *IEEE J Quantum Elect.* 29: 2513–2518, 1993.
33. Knowles, M. R. H. and C. E. Webb, Efficient high-power copper-vapor-laser-pumped Ti:Al_2O_3 laser, *Opt. Lett.* 18: 607–609, 1993.
34. Walling, J. C., High energy pulsed alexandrite lasers. In *Technical Digest International Conference on Lasers '90*, paper MH.3, San Diego, CA, 1990.
35. Imeshev, G. and M. E. Fermann, 230 kW peak power femtosecond pulses from a high-power tunable source based from amplification in Tm-doped fiber, *Opt. Express* 13: 7424–7231, 2005.
36. Fix, A., T. Schröder, R. Wallenstein, J. G. Haub, M. J. Johnson, and B. J. Orr, Tunable β-barium borate optical parametric oscillator: Operating characteristics with and without injection seeding, *J. Opt. Soc. Am. B* 10: 1744–1750, 1993.
37. Maruyama, Y., 0.5-kHz, 5-W optical parametric oscillator pumped by the second harmonic of a Nd:YAG laser, *Opt. Eng.* 44: 094202, 2005.
38. Hollberg, L., CW dye lasers. In F. J. Duarte and L. W. Hillman (Eds), *Dye Laser Principles*, Chapter 5, Academic, New York, 1990.
39. Baving, H. J., H. Muuss, and W. Skolaut, CW dye laser operation at 200 W pump power, *Appl. Phys. B* 29: 19–21, 1982.

40. Adams, C. S. and A. I. Ferguson, Frequency doubling of a single frequency Ti:Al_2O_3 laser using an external enhancement cavity, *Opt. Commun*. 79: 219–223, 1990.
41. Erbert, G., I. Bass, R. Hackel, S. Jenkins, K. Kanz, and J. Paisner, 43-W, CW Ti:sapphire laser, in *Conference on Lasers and Electro-Optics*, pp. 390–393, Optical Society of America, Washington, DC, 1991.
42. Walling, J. C., O. G. Peterson, and R. C. Morris, Tunable CW alexandrite laser, *IEEE J. Quantum Elect*. QE-16: 120–121, 1980.
43. Zorabedian, P., Characteristics of a grating-external-cavity semiconductor laser containing intracavity prism beam expanders, *J. Lightwave Technol*. 10: 330–335, 1992.
44. Fleming, M. W. and A. Moorodian, Spectral characteristics of external-cavity controlled semiconductor lasers, *IEEE J. Quantum Elect*. QE-17: 44–59, 1981.
45. Meng, L. S., B. Nizamov, P. Nadasami, J. K. Brasseur, T. Henshaw, and D. K. Newmann, High-power 7-GHz bandwidth external-cavity diode laser array and its use in optically pumping singlet delta oxygen, *Opt. Express* 14: 10469–10474, 2006.
46. Maulini, R., A. Mohan, M. Giovannini, J. Faist, and E. Gini, External cavity quantum-cascade laser tunable from 8.2 to 10.4 μm using a gain element with a heterogeneous cascade. *Appl. Phys. Lett*. 88: 201113, 2006.
47. Hugi, A., R. Terazzi, Y. Bonetti, A. Wittmann, M. Fischer, M. Beck, J. Faist, and E. Gini, External cavity quantum cascade laser tunable from 7.6 to 11.4 μm, *Appl. Phys. Lett*. 95: 061103, 2009.
48. Bosenberg, W. R., A. Drobshoff, J. I. Alexander, L. E. Myers, and R. L. Byer, 93% pump depletion, 3.5 W continuous-wave, singly resonant optical parametric oscillator, *Opt. Lett.* 21: 1336–1338, 1996.
49. Auerbach, M., P. Adel, D. Wandt, C. Fallnich, S. Unger, S. Jetschke, and H-R. Müller, 10 W widely tunable narrow linewidth double-clad fiber ring laser, *Opt. Express* 10: 139–144, 2002.
50. Shen, D. Y., J. K., Sahu, and W. A. Clarkson, Highly efficient Er, Yb-doped fiber laser with 188 W free running and >100 W tunable output power, *Opt. Express* 13: 4916–4921, 2005.
51. Loree, T. R., K. B. Butterfield, and D. L. Barker, Spectral tuning of ArF and KrF discharge lasers, *Appl. Phys. Lett*. 32: 171–173, 1978.
52. Lyutskanov, V. L., K. G. Khristov, and I. V. Tomov, Tuning the emission frequency of a gas-discharge XeCl laser, *Sov. J. Quantum Electron*. 10: 1456–1457, 1980.
53. Yang, T. T., D. H. Burde, G. A. Merry, D. G. Harris, L. A. Pugh, J. H. Tillotson, C. E. Turner, and D. A. Copeland, Spectra of electron beam pumped XeF laser, *Appl. Opt*. 27: 49–57, 1988.
54. Hofmann, T. and F. K. Tittel, Wideband-tunable high-power radiation by SRS of a XeF($C \rightarrow A$) excimer laser, *IEEE J. Quantum Elect*. 29: 970–974, 1993.
55. Woodward, B. W., V. J. Ehlers, and W. C. Lineberger, A reliable repetitively pulsed, high-power nitrogen laser, *Rev. Sci. Instrum*. 44: 882–887, 1973.
56. Shay, T. M., F. E. Hanson, D. Gookin, and E. J. Schimitscheck, Line narrowing and enhanced efficiency of an HgBr laser by injection locking, *Appl. Phys. Lett*. 39: 783–785, 1981.
57. Bukshpun, L. M., V. V. Zhukov, E. L. Latush, and M. F. Sem, Frequency tuning and mode self locking in He-Sr recombination laser, *Sov. J. Quantum Electron*. 11: 804–805, 1981.
58. Tenenbaum, J., I. Smilanski, S. Gabay, L. A. Levin, G. Erez, and S. Lavi, Structure of 510.6 and 578.2 nm copper laser lines, *Opt. Commun.* 32: 473–477, 1980.
59. Wang, Y., B. Lin, and Y. Qian, Spectral structure of the 627.8 nm gold vapor laser line. *Appl. Phys. B* 49: 149–153, 1989.
60. Duarte, F. J., Variable linewidth high-power TEA CO_2 laser, *Appl. Opt*. 24: 34–37, 1985.

61. Mehendale, S. C., D. J. Biswas, and R. G. Harrison, Single mode multiline emission from a hybrid CO_2 laser, *Opt. Commun.* 55: 427–429, 1985.
62. Chang, T. Y., Vibrational transition lasers. In M. J. Weber (Ed.), *Handbook of Laser Science and Technology*, Chapter 3.3.2, CRC, Boca Raton, FL, 1991.
63. Duarte, F. J., Multiple-prism Littrow and grazing-incidence pulsed CO_2 lasers, *Appl. Opt*. 24: 1244–1245, 1985.
64. Duarte, F. J., Introduction. In F. J. Duarte (Ed.), *Tunable Laser Applications*, 1st edn, Chapter 1, Marcel-Dekker, New York, 1995.
65. Duarte, F. J., Introduction. In F. J. Duarte (Ed.), *Tunable Lasers Handbook*, Chapter 1, Academic, New York, 1995.
66. Farkas, A. M. and J. G. Eden, Pulsed dye amplification and frequency doubling of single longitudinal mode semiconductor, *IEEE J. Quantum Elect.* 29: 2923–2927, 1993.
67. Duarte, F. J., Solid-state multiple-prism grating dye-laser oscillators, *Appl. Opt.* 33: 3857–3860, 1994.
68. Orr, B. J., Private communication, 1995.
69. Andersen, T. V., O. Schmidt, C. Bruchmann, J. Limpert, C. Aguergaray, E. Cormier, and A. Tünnermann, High repetition rate tunable femtosecond pulses and broadband amplification from fiber laser pumped parametric amplifier, *Opt. Express* 14: 4765–4773, 2006.
70. Eichhorn, M., Development of a high-pulse-energy Q-switched Tm-doped double-clad fluoride fiber laser and its application to the pumping of mid-IR lasers, *Opt. Lett.* 32: 1056–1058, 2007.
71. Duarte, F. J., Letter, *Laser Focus World* 27(5): 25, 1991.
72. Duarte, F. J., Letter, *Lasers Optron.* 10(5): 8, 1991.
73. Drell, P. S. and E. D. Commins, Parity nonconservation in atomic thallium, *Phys. Rev. A* 32: 2196–2210, 1985.
74. Gould, P. L., G. A. Ruff, and D. E. Pritchard, Diffraction of atoms by light: The near-resonant Kapitza-Dirac effect, *Phys. Rev. Lett*. 56: 827–830, 1986.
75. Letokhov, V. S., Atomic optics with tunable dye lasers. In M. Stuke (Ed.), *Dye Lasers: 25 Years*, Chapter 11, Springer, Berlin, 1992.
76. Hall, R. J. and A. C. Eckbreth, Coherent anti-Stokes Raman spectroscopy, CARS: Application to combustion diagnostics. In J. F. Ready and R. K. Erf (Eds), *Laser Applications*, Volume 5, Chapter 4, Academic, New York, 1984.
77. Majewski, W. A., J. F. Pfanstiel, D. F. Plusquellic, and W. D. Pratt, High resolution optical spectroscopy in the ultraviolet. In A. B. Myers and T. R. Rizzo (Eds), *Laser Techniques in Chemistry*, Chapter 4, Wiley, New York, 1995.
78. Sneddon, J., T. L. Thiem, and Y-I. Lee (Eds), *Lasers in Analytical Atomic Spectroscopy*, Wiley-VCH, New York, 1996.
79. Demtröder, W., *Laserspektroscopie: Grundlagen und Techniken*, Springer, Berlin, 2007.
80. Pease, A. A. and W. M. Pearson, Axial-mode structure of a copper vapor pumped dye laser, *Appl. Opt.* 16: 57–60, 1977.
81. Hargrove, R. S. and T. Kan, High power efficient dye amplifier pumped by copper vapor lasers, *IEEE J. Quantum Elect.* 16: 1108–1113, 1980.
82. Duarte, F. J. and J. A. Piper, Comparison of prism-expander and grazing-incidence grating cavities for copper laser pumped dye lasers, *Appl. Opt.* 21: 2782–2786, 1982.
83. Duarte, F. J. and J. A. Piper, Narrow-linewidth, high-prf copper laser-pumped dye-laser oscillators, *Appl. Opt.* 23: 1391–1394, 1984.
84. Broyer, M. and J. Chevaleyre, CVL-pumped dye laser for spectroscopic applications, *Appl. Phys. B* 35: 31–36, 1984.
85. Paisner, J. A. and R. W. Solarz, Resonance photoionization spectroscopy. In L. J. Radziemski, R. W. Solarz, and J. A. Paisner (Eds), *Laser Spectroscopy and Its Applications*, Chapter 3, Marcel Dekker, New York, 1987.

86. Paisner, J. A., Atomic vapor laser isotope separation, *Appl. Phys. B* 46: 253–260, 1988.
87. Duarte, F. J., H. R. Aldag, R. W. Conrad, P. N. Everett, J. A. Paisner, T. G. Pavlopoulos, and C. R. Tallman, High power dye laser technology. In R. C. Sze and F. J. Duarte (Eds), *Proceedings of the International Conference on Lasers '88*, pp. 773–790. STS, McLean, VA, 1989.
88. Akerman, M. A., Dye-laser isotope separation. In F. J. Duarte and L. W. Hillman (Eds), *Dye Laser Principles*, Chapter 9, Academic, New York, 1990.
89. Duarte, F. J., Dispersive dye lasers. In F. J. Duarte (Ed.), *High Power Dye Lasers*, Chapter 9, Springer, Berlin, 1991.
90. Tallman, C. and R. Tennant, Large-scale excimer-laser-pumped dye lasers. In F. J. Duarte (Ed.), *High Power Dye Lasers*, Chapter 4, Springer, Berlin, 1991.
91. Webb, C. E., High-power dye lasers pumped by copper-vapor lasers. In F. J. Duarte (Ed.), *High Power Dye Lasers*, Chapter 5, Springer, Berlin, 1991.
92. Singh, S., K. Dasgupta, S. Kumar, K. G. Manohar, L. G. Nair, and U. K. Chatterjee, High-power high-repetition-rate copper-vapor-pumped dye laser, *Opt. Eng.* 33: 1894–1904, 1994.
93. Sugiyama, A., T. Nakayama, M. Kato, Y. Maruyama, and T. Arisawa, Characteristics of a pressure-tuned single-mode dye laser oscillator pumped by a copper vapor laser, *Opt. Eng.* 35: 1093–1097, 1996.
94. Ready, J. F., *Industrial Laser Applications*, Academic, New York, 1997.
95. Bokhan, P. A., V. V. Buchanov, N. V. Fateev, M. M. Kalugin, M. A. Kazaryan, A. M. Prokhorov, and D. E. Kakrevskii, *Laser Isotope Separation in Atomic Vapor*, Wiley-VCH, Weinheim, 2006.
96. Klick, D., Industrial applications of dye lasers. In F. J. Duarte and L. W. Hillman (Eds), *Dye Laser Principles*, Chapter 8, Academic, New York, 1990.
97. Hargrove, R. S., Industrial applications of high power lasers. In *Technical Digest International Conference on Lasers '91*, paper THA.2, San Diego, CA, 1991.
98. Browell, E. V., Ozone and aerosol measurements with an airborne lidar system, *Opt. Photonics News* 2(10): 8–11, 1991.
99. Grant, W. B., Lidar for atmospheric and hydrospheric studies. In F. J. Duarte (Ed.), *Tunable Laser Applications*, 1st edn, pp. 213–305, Marcel-Dekker, New York, 1995.
100. Duarte, F. J., Organic dye lasers: Brief history and recent developments, *Opt. Photonics News* 14(10): 20–25, 2003.
101. Goldman, L., Dye lasers in medicine. In F. J. Duarte and L. W. Hillman (Eds), *Dye Laser Principles*, Chapter 10, Academic, New York, 1990.
102. Vassen, W., C. Zimmermann, R. Kallenbach, and T. W. Hänsch, A frequency-stabilized titanium sapphire laser for high-resolution spectroscopy, *Opt. Commun.* 75: 435–440, 1990.
103. Gilmore, D. A., P. V. Cvijin, and G. H. Atkinson, Intracavity absorption spectroscopy with a titanium:sapphire laser, *Opt. Commun.* 77: 385–389, 1990.
104. Bruneau, D., T. Arnaud des Lions, P. Quaglia, and J. Pelon, Injection-seeded pulsed alexandrite laser for differential absorption Lidar application, *Appl. Opt.* 33: 3941–3950, 1994.
105. Diddams, S. A., D. J. Jones, J. Ye, S. T. Cundiff, J. L. Hall, J. K. Ranka, R. S. Windeler, et al., Direct link between microwave and optical frequencies with 300 THz femtosecond laser comb, *Phys. Rev. Lett.* 84: 5102–5105, 2000.
106. Holzwarth, R., Th. Udem, T. W. Hänsch, J. C. Knight, W. J. Wadsworth, and P. S. J. Russell, Optical frequency synthesizer for precision spectroscopy, *Phys. Rev. Lett.* 85: 2264–2267, 2000.
107. Camparo, J. C., The diode laser in atomic physics, *Contemp. Phys.* 26: 443–477, 1985.
108. Wieman, C. E. and L. Hollberg, Using diode lasers in atomic physics, *Rev. Sci. Instrum.* 62: 1–20, 1991.

109. Camparo, J., The rubidium atomic clock and basic research, *Phys. Today* 60(11): 33–39, 2007.
110. Weidemüller, M., C. Gabbanini, J. Hare, M. Gross, and S. Haroche, A beam of laser-cooled lithium Rydberg atoms for precision microwave spectroscopy, *Opt. Commun*. 101: 342–346, 1993.
111. Atutov, S. N., E. Mariotti, M. Meuchi, C. Marinelli, and L. Moi, 670 nm external-cavity single mode diode laser continuously tunable over 18 GHz range, *Opt. Commun*. 107: 83–87, 1994.
112. Myatt, C. J., N. R. Newbury, R. W. Ghrist, S. Loutzenhizer, and C. E. Wieman, Multiply loaded magneto-optical trap, *Opt. Lett.* 21: 290–292, 1996.
113. Olivares, I. E., A. E. Duarte, E. A. Saravia, and F. J. Duarte, Lithium isotope separation with tunable diode lasers, *Appl. Opt.* 41: 2973–2977, 2002.
114. Berger, J. D. and D. Anthon, Tunable MEMS devices for optical networks, *Opt. Photonics News* 14(3): 43–49, 2003.
115. Duarte, F. J. (Ed.), *Tunable Laser Applications*, 1st edn, Marcel-Dekker, New York, 1995.
116. Duarte, F. J. (Ed.), *Tunable Laser Applications*, 2nd edn, CRC Press, New York, 2009.
117. Duarte, F. J. (Ed.), *Tunable Laser Applications*, 3rd edn, CRC Press, New York, 2015.

This page intentionally left blank

2 Spectroscopic Applications of Tunable Optical Parametric Oscillators

Brian J. Orr, John G. Haub, Yabai He, and Richard T. White

CONTENTS

2.1 INTRODUCTION

2.1.1 "Good-bye to Ti: and Dye"?

The corresponding chapter in the first edition of this book [1] was written in the mid-1990s, at a time when a prominent scientific laser manufacturer had advertised its latest optical parametric oscillator (OPO) with the motto "Good-bye to Ti: and Dye," signaling the possible demise of tunable dye lasers that had served laser spectroscopists and others well for at least 20 years [2,3]. At that time, a book review speculated that solid-state tunable lasers "might relegate the dye laser to the pages of the history book," counterpoised by a view that "the dye laser in its many incarnations looks set to be with us for quite some time yet" [4]. Approximately 15 years later, the corresponding chapter in the second edition of this book [5] recorded that Ti:sapphire and dye lasers continued to occupy a significant place in the tunable laser market alongside many others (such as diode and quantum cascade lasers), but that solid-state nonlinear optical (NLO) devices, such as OPOs, were by then preferred as tunable coherent light sources for many spectroscopic purposes in the ultraviolet (UV), visible, near-infrared (IR), and mid-IR [6,7]. The same is true at the time of preparation of this updated chapter (~20 and ~5 years, respectively, after our contributions to the first [1] and second [5] editions of this book), although the spectroscopic dye laser market continues to contract substantially.

This chapter focuses on developments in the design, operation, and spectroscopic applications of tunable OPOs, as well as in the closely related optical parametric generator (OPG) and optical parametric amplifier (OPA) devices. Such optical parametric devices have now been available for more than 40 years [8,9], but it is only in the last 25 years that the spectroscopic community at large has found tunable OPOs to be sufficiently reliable for routine, trouble-free operation. Pulsed OPO devices operating in the nanosecond (ns) regime had long been recognized as potentially useful sources of broadly tunable, coherent radiation for spectroscopy, typically yielding high peak and average powers [8–12]. Their solid-state character and high

efficiency offer substantial advantages in some respects over the previously ubiquitous dye laser. Moreover, the wide range of wavelengths over which many OPOs can be tuned has opened up prospects for laser spectroscopy in otherwise inaccessible spectral regions, such as the near- and mid-IR, on which much of this chapter will concentrate [6,7].

The first precursor of this chapter [1] displayed an IR absorption spectrum of the 2–0 first-overtone band of carbon monoxide (CO) gas in the near IR at ~2.35 μm; that spectrum was remarkably fine by the standards that prevailed when it was recorded in 1972 (over 40 years ago), using idler radiation from an ns-pulsed, singly resonant $LiNbO_3$ OPO [10,13]. The spectrum displayed in Figure 2.1 shows the P ($\Delta J = -1$) and R ($\Delta J = +1$) branches of that rovibrational band, spanning a 180 cm^{-1} (5.4 THz) range with an instrument-limited linewidth of ~0.5 cm^{-1} (~15 GHz) at a CO sample pressure (P) of 3 atm in a 4 cm cell. It was accompanied by a (subsequently fulfilled) prophecy that "the use of parametric oscillator sources for molecular spectroscopy should increase rapidly as the frequency range is extended further into the IR and the bandwidth is reduced" [10].

Within 2 years, Stanford University's OPO technology had further advanced: pulsed $LiNbO_3$ OPO idler radiation, continuously tunable with an optical bandwidth of 0.35 cm^{-1} (10.5 GHz), enabled better-resolved reference spectra of the same 2.35 μm 2–0 band of CO gas to be recorded [14]. These were used in the context of an OPO-based transmitter–receiver system that was able to detect CO in air at a range of 107 m against a topographical backscattering target, providing an early

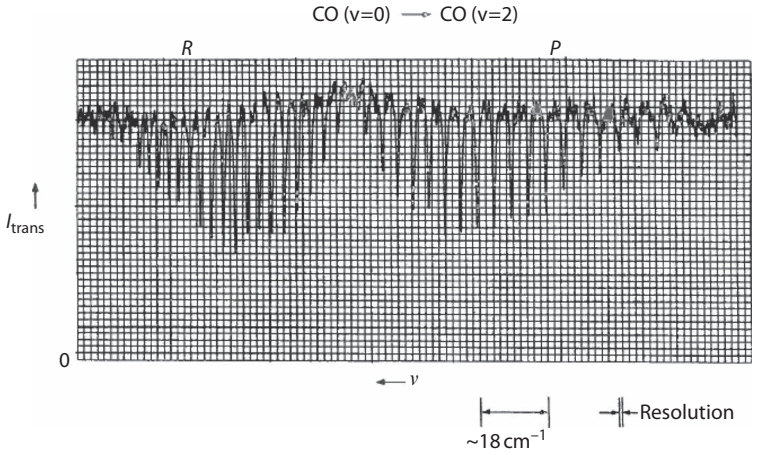

FIGURE 2.1 Continuously scanned IR absorption spectrum of the 2.35 μm 2–0 rovibrational absorption band of carbon monoxide (CO) gas, recorded in a 4 cm cell at a pressure of 3 atm using an ns-pulsed, singly resonant $LiNbO_3$ OPO: an early demonstration of the spectroscopic potential of tunable OPO technology [10,13]. (Reproduced with permission from R. L. Byer, Optical parametric oscillators. In H. Rabin and C. L. Tang (Eds), *Quantum Electronics: A Treatise*, Volume I, Part B, Chapter 9, pp. 578–702, Academic, New York, 1975; Sackett, P. (US Air Force Cambridge Research Laboratory), cited in [10] as a private communication to R. L. Byer (1972).

indication of the utility of OPO-based IR spectroscopy for stand off detection and density measurement of pollutant gases [15].

However, despite some significant early progress, the spectroscopic potential of pulsed OPOs was not readily realized [9–12,14,16]. Many research laboratories had dark recesses to which their original pulsed OPO systems had been relegated, either optically damaged or used occasionally as "one-wavelength-at-a-time" instruments, rather than the continuously scannable spectroscopic workhorses that they were originally intended to be (and have now become). This shortcoming was attributable to several critical factors:

- The low optical damage limits and high oscillation thresholds in available OPO gain materials.
- The relative complexity of early pulsed OPO cavity designs (including phase-matching schemes and line-narrowing strategies) necessary to achieve narrowband, continuously tunable operation [6,9,10,17–23].
- The need for intense, pulsed lasers with adequate temporal and spatial coherence to serve as OPO pump sources.

Within the last 25 years, these problems have diminished appreciably with the availability of new OPO materials [24,26] and high-quality pump lasers [27]. As a variety of pulsed tunable OPO systems became commercially available, the spectroscopic community, sections of which had in earlier days been disappointed by the difficulty of implementing OPO technology, were attracted to the cost-effectiveness and practical utility of such systems.

Since the first edition of this book [1], tunable OPOs, their applications, and relevant aspects of nonlinear optics have matured considerably. There have been numerous review articles, both by our research group at Macquarie University, Sydney [28–33] and by others [34–59], as well as relevant feature issues of topical journals on OPOs [60–67] and related spectroscopic techniques [68–70]. In this chapter, therefore, we do not intend to provide a comprehensive coverage of the field, but, rather, to indicate some of its foundations and address a number of issues concerning the design and operation of tunable OPOs for various spectroscopic applications. This overview will include continuous wave (CW) and ultrafast pulsed systems, as well as the ns-pulsed devices on which our earlier versions of this chapter [1,5] and our own ongoing research have focused. Our approach here is essentially that of a selective series of case studies sampling representative examples of progress in this area.

2.1.2 OPO-Based Spectroscopy Has Come a Long Way …

OPO-based spectroscopy has come a long way since 1972, when Figure 2.1 was recorded. To illustrate how far this field has progressed, we retain CO molecular studies as a benchmark and examine several more recent OPO-spectroscopic accomplishments (but without many technological details at this introductory stage of the chapter).

For instance, a diode-pumped CW OPO with an optical linewidth of <60 MHz was used in 1999 to measure higher-resolution spectra of CO ($P = 4$ Torr) in a single

pass of a 60 cm gas cell; the 2.3337 μm $R(6)$ rovibrational line of CO (in the same 2–0 band as in Figure 2.1) was recorded with a Doppler- and pressure-broadened linewidth of 0.013 cm^{-1} (390 MHz) [71]. Around the same time, an advanced, commercially available, computer-controlled tunable OPO/OPA system (based on the ns-pulsed design of Bosenberg and Guyer [20,21]) was used for IR planar laser-induced fluorescence (LIF) imaging of fluid dynamics in CO gas flows and of CO combustion diagnostics [72–74]. Figure 2.2 shows a single-shot planar LIF image of a vortex in a CO/Ar gas jet [72].

Our ultimate illustration of the extensive recent progress in this field, still in the context of molecular spectroscopy of CO(g), is provided by recent work of Vodopyanov and colleagues [75,76]. They have developed state-of-the-art broadband OPOs operating in the spectral range 2.5–5 μm for intracavity spectroscopy with sub-parts per million by volume (ppmv) detection limits for various gases, including CO, for which a mid-IR spectrum is shown in Figure 2.3. The black trace is an absorption spectrum measured within 2 min for 50 parts ppmv of CO in He at $P = 1$ atm. In the calculated spectrum (gray; offset and inverted), the effective path length is taken to be seven times the physical length (48 cm) of the intracavity gas cell.

Figure 2.4 illustrates the layout of the degenerate broadband OPO that was used. The pump source is a femtosecond (fs) fiber laser, either Er doped operating at 1.56 μm or Tm doped operating at 2.05 μm. The corresponding NLO material is either periodically poled lithium niobate (PPLN) or orientation-patterned gallium arsenide (OP GaAs); wedge pairs composed of either ZnSe or CaF_2 are used for dispersion compensation and beam out-coupling.

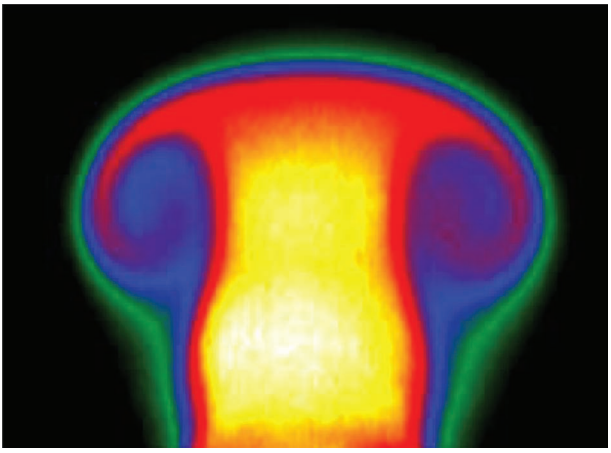

FIGURE 2.2 Single-shot IR planar laser-induced fluorescence image of a vortex in a CO/Ar gas jet, formed by releasing a 50:50 mixture of CO and Ar through a 6 mm tube into air [72]. A computer-controlled tunable OPO/OPA system operating at ~2.35 μm was used to excite CO molecules via their near IR 2–0 overtone absorption band (the same as in Figure 2.1), and then 2–1 and 1–0 fundamental-band mid-IR emission was detected at ~4.7 μm. (With kind permission from Professor R. K. Hanson and Springer Science+Business Media: B. J. Kirby and R. K. Hanson, Planar laser-induced fluorescence imaging of carbon monoxide using vibrational (infrared) transitions, *Appl. Phys. B* 69: 505–507, 1999.)

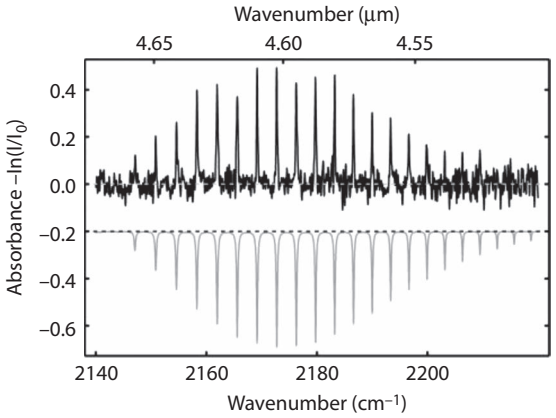

FIGURE 2.3 Comparison of measured (black) and calculated (gray) mid-IR rovibrational absorption spectra at ~4.6 μm for 50 ppmv CO in He at 1 atm pressure. The spectra correspond to the *R* branch of the 1–0 fundamental band of CO gas at ~4.6 μm, observed by means of an fs-pumped broadband frequency comb OPO incorporating an intracavity gas cell, as depicted in Figure 2.4 [75]. (From M. W. Haakestad, T. P. Lamour, N. Leindecker, A. Marandi, and K. L. Vodopyanov, Intra-cavity trace molecular detection with a broadband mid-IR frequency comb source, *J. Opt. Soc. Am. B* 30: 631–640, 2013. With permission from Professor K. L. Vodopyanov and Optical Society of America.)

The approach represented by Figures 2.3 and 2.4 is in marked contrast to that of more traditional OPO-spectroscopic techniques, in several respects [75,76]:

- Many traditional OPO-spectroscopic studies use a narrow-bandwidth source, of which the tunable output wavelength (signal or idler) is either scanned through the spectrum of interest (as in Figure 2.1 [10,13] and in other examples cited in previous references [14,15,71]) or tuned to a single characteristic spectroscopic feature (as in Figure 2.2 [72–74]). However, here the fs-pumped broadband OPO, together with Fourier-transform (FT) methods, is able to record an entire spectrum without needing to continuously tune or select the OPO output wavelength.
- All of the previously considered examples of OPO spectroscopy have focused on near IR absorption at ~2.35 μm in the 2–0 first-overtone absorption band of CO gas (as in Figure 2.1 and cited in previous references [10,13–15,71–74]), due to the limited long-wavelength range of idler radiation from readily available OPO NLO media and ns-pulsed pump lasers. By contrast, the use of an OP GaAs OPO fs-pumped by a 2.05 μm Tm-doped fiber laser provides broadband spectroscopic access to the much stronger 1–0 fundamental band of CO gas at ~4.6 μm; the rovibrational *R* branch of that spectrum is displayed in Figure 2.3. Innovative aspects of OP GaAs as a relatively new NLO medium are further considered later in this chapter (e.g., in Section 2.2.3).
- The instrument shown in Figure 2.4 comprises a doubly resonant, degenerate OPO that is synchronously pumped [75,76]. The spectrum of its fs-pump

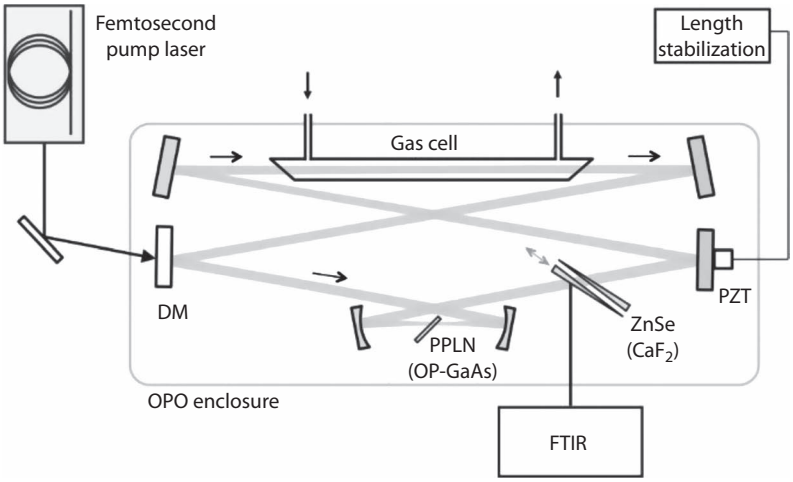

FIGURE 2.4 Schematic layout of the degenerate broadband OPO used to measure the mid-IR 1–0 fundamental-band absorption spectrum (as in Figure 2.3) of CO gas contained in an intracavity cell [75]. In that application, the pump beam from an fs-pulsed Tm-doped fiber laser (operating at 2.05 μm) was introduced through an in-coupling dielectric mirror DM; the other five mirrors were gold coated. A pair of CaF_2 wedges (for dispersion compensation and mid-IR beam out-coupling) were used, and the nonlinear optical crystal was OP-GaAs (placed at Brewster's angle) to generate a broadband frequency comb output spectrum centered at ~4.1 μm. Alternative shorter-wavelength applications (with an output spectrum centered at ~3.4 μm) have employed a 1.56 μm Er-doped fiber laser, a ZnSe wedge pair, and an AR-coated PPLN nonlinear optical crystal. (From M. W. Haakestad, T. P. Lamour, N. Leindecker, A. Marandi, and K. L. Vodopyanov, Intra-cavity trace molecular detection with a broadband mid-IR frequency comb source, *J. Opt. Soc. Am. B* 30: 631–640, 2013. With permission from Professor K. L. Vodopyanov and Optical Society of America.)

frequency comb is downconverted with high fidelity, thereby generating mid-IR frequency combs with large parametric gain bandwidth. Extensive mixing of comb components results in an extremely large instantaneous mid-IR bandwidth that spans more than one octave and is suitable for molecular spectroscopy at wavelengths out to ~6 μm.

- The spectroscopic sensitivity of this broadband mid-IR source is enhanced for trace gas detection by coupling the frequency comb into a high-finesse Fabry–Perot cavity to attain long effective optical path lengths and conveniently short measurement times. This has been realized for the following six trace gases (with reported detection limits, all diluted at 1 atm pressure, at chosen operating wavelengths): methane (CH_4, 1.7 parts per billion by volume [ppbv] at ~3.3 μm), formaldehyde (H_2CO, 0.31 ppmv at ~3.5 μm), acetylene (C_2H_2, 0.11 ppmv at ~3.0 μm), ethylene (C_2H_4, 0.32 ppmv at ~3.3 μm), CO (0.27 ppmv at ~4.8 μm), and isotopic carbon dioxide ($^{13}CO_2$, 2.4 ppbv at ~4.4 μm) [75,76]. The two longer-wavelength intracavity measurements (of CO in He and of $^{13}CO_2$ in ambient air) employed the OP GaAs OPO system with a Tm-doped fiber laser pump, while the other four (at

shorter wavelengths, in N_2) employed the PPLN OPO system pumped by an Er-doped fiber laser, as in Figure 2.4.

- In these OPO-spectroscopic measurements, the line shapes are found to have dispersive features (e.g., as for CO in the upper trace of Figure 2.3), which can be adequately described by a model that takes into account intracavity passive loss and round-trip group delay dispersion across the broad OPO frequency band.

The foregoing five bullet points, together with Figures 2.3 and 2.4, provide a representative demonstration of the significant scale of technological and scientific advances that continue to be made in the area of OPO-based spectroscopy [75,76].

2.2 OPTICAL PARAMETRIC DEVICES: HOW THEY OPERATE

2.2.1 Optical Parametric Processes

Optical parametric devices are useful sources of coherent, laser-like radiation that are typically intense and tunable over a wide range of wavelengths. They invariably arise via nonlinear optics, most frequently through a three-wave mixing process mediated by the NLO susceptibility tensor $\boldsymbol{\chi}^{(2)}$ in a noncentrosymmetric crystalline medium [77–80]. Three forms of optical parametric device are illustrated in Figure 2.5: (a) OPG, (b) OPA, and (c) OPO. Also illustrated is a closely related (but distinct) NLO device: (d) the difference-frequency generator (DFG). Coherent light waves are represented by arrows, with their associated optical angular frequency ω_j and wave vector $\mathbf{k}_j$ (as defined later in this section). In Figure 2.5, input and output waves are shown as arrows on the left and right, respectively, with their breadth indicating typical relative intensities.

An OPG is the simplest form of optical parametric device. As depicted in Figure 2.5a, it entails a single input wave (pump P, at frequency ω_P) and two output waves: signal S (at ω_S) and idler I (at ω_I), where $\omega_S \geq \omega_I$. The NLO process itself is initiated by spontaneous parametric processes that comprise naturally occurring emission/noise/fluorescence at low intensity, effectively "splitting" a pump photon into two new photons [81]. There is considerable interest in *spontaneous parametric downconversion* at the single-photon level, in view of its relevance to quantum optics, quantum entanglement, and quantum computing [82,83]. However, for relatively high-power optical parametric generation as considered here, a semiclassical description can be retained without quantum-optical subtleties [81].

Once a signal or idler wave has been generated, it can be coherently amplified by passing it through an OPA together with input pump radiation, as depicted in Figure 2.5b. A further order of sophistication is reached in an OPO, as depicted in Figure 2.5c, in which the functions of an OPG and an OPA are combined by multipassing one or more of the optical waves involved inside a resonant optical cavity, formed by two or more appropriately aligned reflectors (M_1, M_2).

A DFG, as depicted in Figure 2.5d, is *not* an optical parametric device, although the DFG source term is central to the NLO mechanism of OPGs, OPAs, and OPOs. In a DFG, two intense input waves (with frequencies ω_1 and ω_2) interact coherently to generate a third output wave (with frequency ω_{diff}) at the difference frequency

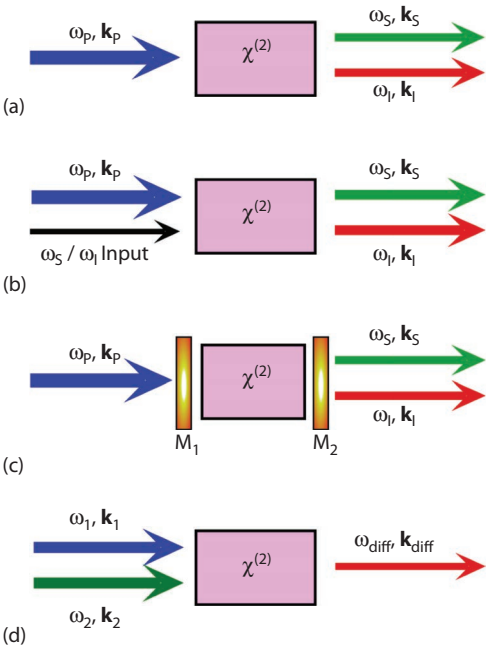

FIGURE 2.5 Schematic diagrams of three forms of optical parametric device. (a) Optical parametric generator (OPG). (b) Optical parametric amplifier (OPA). (c) Optical parametric oscillator (OPO). Note that, by convention, optical frequencies of the signal (S) and idler (I) output waves are defined such that $\omega_S \geq \omega_I$. Also shown is a fourth closely related device: (d) Difference-frequency generator (DFG). Nonlinear optical (NLO) media are denoted by their susceptibility tensor $\boldsymbol{\chi}^{(2)}$. Arrows represent input and output waves, together with their optical frequencies ω_j and wave vectors $\mathbf{k}_j$. An OPO requires an optical resonator, comprising at least two aligned reflectors (M_1, M_2).

of the two input waves [11,84]. There are now two relatively high-power driving waves (rather than one), and the frequencies of these waves are subtracted from each other (rather than effectively splitting a single incident frequency in two, as in an optical parametric process). Nevertheless, the outcome and utility of a DFG can be similar to those of an optical parametric device. For instance, if coherent radiation is required at a particular IR wavelength, it can be generated either as the idler wave of an optical parametric device, with frequency $\omega_I = (\omega_P - \omega_S)$, or as the output wave of a DFG, with frequency $\omega_{diff} = |\omega_1 - \omega_2|$. Moreover, the NLO source term for a DFG entails a form of susceptibility tensor $\boldsymbol{\chi}^{(2)}$ that is very similar to that for an OPG, OPA, or OPO. Furthermore, the mechanistic description of a DFG, as in Figure 2.5d, converges on that of an OPA, as in Figure 2.5b, when the field strength of the signal or idler input wave in the OPA case is increased to approach that of its pump wave.

Many desirable attributes of optical parametric devices in general, and tunable OPOs in particular, arise from the fact that any such instrument is derived from nonlinear optics [77–80] and is therefore distinctively different from a laser. This yields flexible, versatile design features, such as modes of temporal and wavelength control

to which lasers are not amenable. Lasers generally depend on population inversion of an optical gain medium, with associated optical lifetime and saturation limitations. On the other hand, optical parametric gain, oscillation, and amplification facilitate modular system design because they entail NLO coefficients and phase-matching conditions, as explained in this section.

In nonlinear optics, a number (σ, >2) of optical waves interact in a medium with NLO susceptibility tensor $\boldsymbol{\chi}^{(\sigma-1)}$. For inelastic optical processes, these waves (with angular frequencies ω_1, ω_2,…, ω_σ) obey two *conservation conditions*. One is for energy (or frequency):

$$\omega_1 + \omega_2 + \cdots + \omega_\sigma = 0 \tag{2.1}$$

The other conservation condition is effectively for momentum; this is expressed in terms of wave vectors $\mathbf{k}_j$ (with $j = 1, 2, \ldots, \sigma$) that have magnitudes $k_j = n_j \omega_j / c = 2\pi n_j / \lambda_j$, where n_j is the refractive index at vacuum wavelength λ_j, and c is the speed of light:

$$\mathbf{k}_1 + \mathbf{k}_2 + \cdots + \mathbf{k}_\sigma + \Delta\mathbf{k} = 0 \tag{2.2}$$

where $\Delta\mathbf{k}$ is the phase-mismatch vector between the σ interacting waves. Each frequency component ω_j and wave vector $\mathbf{k}_j$ is ascribed a positive or a negative sign, according to its phase relationships. Equation 2.2 defines a phase-matching condition, in which $\Delta\mathbf{k}$ must be minimized to optimize the efficiency of the NLO process of interest.

Two specific three-wave NLO processes that are relevant to this chapter are those for either an optical parametric device (i.e., OPG, OPA, or OPO) or a DFG. Each of these is mediated by the second-order NLO susceptibility tensor $\boldsymbol{\chi}^{(2)}$, which is nonzero in a crystalline medium only if it is noncentrosymmetric. Many such crystals are available [24,25]. For example, lithium niobate ($LiNbO_3$) has been popular since the early days of pulsed tunable OPOs. Subsequent interest and activity in optical parametric device technology have been stimulated by the availability of NLO materials such as BBO (β-barium borate, BaB_2O_4) and KTP (potassium titanyl phosphate, $KTiOPO_4$). Much impetus has come from quasi-phase-matched (QPM) NLO media, such as periodically poled (PP) materials PPLN and PPKTP, tailored for specific wavelengths by the periodic structuring of ferroelectric domains. QPM media offer compact, efficient, low-threshold alternatives to conventional birefringently phase-matched (BPM) media. The characteristics of many BPM and QPM NLO crystalline media are accessible, both in books [24,25] and via the versatile SNLO software package [26].

For a three-wave optical parametric device, which is of principal interest in this chapter, the energy and momentum conservation conditions of Equations 2.1 and 2.2 become

$$\omega_P - \omega_S - \omega_I = 0; \quad \mathbf{k}_P - \mathbf{k}_S - \mathbf{k}_I - \Delta\mathbf{k} = 0 \tag{2.3}$$

where a laser input wave ("pump," frequency ω_P, wave vector $\mathbf{k}_P$) yields two coherent output waves ("signal," ω_S, $\mathbf{k}_S$; "idler," ω_I, $\mathbf{k}_I$), such that $\omega_P > \omega_S \geq \omega_I$. Note that the

idler frequency ω_I equals the difference ($\omega_P - \omega_S$) between pump and signal frequencies. Equation 2.3 should be viewed in the context of parts (a–c) of Figure 2.5.

Equation 2.2 and the second half of Equation 2.3 apply strictly only to the conventional case of BPM media. In such media, the phase-matching condition $\Delta\mathbf{k} \approx 0$ is attained by adjusting its ordinary- and extraordinary-ray refractive indices via the angle and temperature of a birefringent NLO crystal. Such adjustments are used to optimize parametric conversion efficiency for a particular set of frequencies (ω_P, ω_S, ω_I) and thereby control the output signal and idler wavelengths, λ_S and λ_I. If it is assumed that the three waves are collinear and $\Delta\mathbf{k}$ is exactly zero, then the signal frequency/wavelength is given simply in terms of the pump frequency/wavelength and the refractive indices n_j ($j = P, S, I$) as

$$\omega_S = \omega_P \frac{(n_P - n_I)}{(n_S - n_I)}; \quad \lambda_S = \lambda_P \frac{(n_S - n_I)}{(n_P - n_I)} \tag{2.4}$$

Various angle-dependent index-matching schemes are applicable in the case of OPOs based on BPM crystals: for example, Type I (eeo/ooe) and Type II (oeo/eoe) in positive/negative uniaxial birefringent crystals, where "o" and "e" denote the ordinary and extraordinary waves listed in the order "I S P" [24,84]. Many BPM optical parametric devices (especially those in the ns-pulsed regime) employ so-called critical phase matching (CPM, which may be either collinear or noncollinear), which depends on the orientation of the optical-wave propagation directions relative to the optic axis of the NLO crystal [10,11,24,43,47,48,84].

An alternative approach is so-called noncritical phase matching (NCPM, also known as 90° phase matching), in which the propagation direction is normal to the optic axis of the NLO crystal, and the ordinary- and extraordinary-wave refractive indices n_o and n_e have a zero first-order dependence on the orientation of the crystal [10,11,24,43,47,48,84]. NCPM enables the phase-matched interaction to be along a principal optical axis of the NLO material with no spatial walk-off. This also has the advantage that the effective interaction length is determined by the length of the crystal and is not reduced by spatial walk-off. For a fixed pump wavelength, the output signal and idler wavelengths of an NCPM OPO can then be tuned by varying the temperature (and hence the refractive indices) of the crystal at a fixed (90°) orientation. Alternatively, NCPM OPO output can be tuned by varying the pump wavelength (e.g., from a tunable dye or Ti:sapphire laser—so much for "Good-bye to Ti: and Dye," as proclaimed in Section 2.1.1 [1,5]), while maintaining the fixed crystal temperature and orientation. Such a NCPM approach was popular in the early days of OPO spectroscopy [10,11,16,17] and has since seen a resurgence, particularly for CW OPOs or for ultrafast OPOs, in which the absence of beam walk-off facilitates tight focusing of the (relatively low-power) CW or ultrafast pump beam to exceed the threshold of the OPO (as discussed in Sections 2.3.2 and 2.3.3).

The QPM approach was first recognized by pioneers of nonlinear optics in 1962 as an alternative to birefringent phase matching [85–87]. However, this QPM approach was not realized practically until ~30 years later, via NLO media such as PPLN [49,50,88–92]. For a QPM device, grating contributions, arising from the

engineered microscale structure of the crystal, need to be included in phase-matching conditions. For instance, the z-component Δk of the wave-vector mismatch $\Delta\mathbf{k}$ in the second half of Equation 2.3 needs to be replaced by $\Delta k = [\Delta k_{QPM} + (2\pi\, m/\Lambda)]$, where m is the QPM order (usually an odd-numbered integer), Λ is the QPM grating period, and a collinear interaction along the z-axis is assumed.

In the corresponding case of a DFG (which, we repeat, is *not* an optical parametric device), two coherent input waves (frequencies ω_1, ω_2; wave vectors $\mathbf{k}_1$, $\mathbf{k}_2$) yield a single coherent output wave at the difference frequency $\omega_{diff} = |\omega_1 - \omega_2|$ (with wave vector $\mathbf{k}_{diff}$). The energy and momentum conservation conditions of Equations 2.1 and 2.2 then become

$$\left|\omega_1 - \omega_2\right| - \omega_{diff} = 0; \quad \mathbf{k}_1 - \mathbf{k}_2 - \mathbf{k}_{diff} - \Delta\mathbf{k} = 0 \tag{2.5}$$

as depicted in Figure 2.5d. As in Equations 2.2 and 2.3, phase matching is achieved when $\Delta\mathbf{k} \approx 0$ for BPM media. In the case of QPM media, there is an additional grating contribution in the second half of Equation 2.5, in which the z-component Δk of the vector $\Delta\mathbf{k}$ in the second half of Equation 2.3 needs to be replaced by $\Delta k = [\Delta k_{QPM} + (2\pi\, m/\Lambda)]$.

In a general sense (which is incidental to this chapter), other important forms of coherent wavelength conversion arise from four-wave mixing processes that are mediated by the third-order NLO susceptibility tensor $\chi^{(3)}$, which can be nonzero even in isotropic or centrosymmetric media such as gases, liquids, optical fibers, and all classes of crystal. Optical parametric processes of this type contribute to stimulated Raman scattering (SRS), involving an optical medium with Raman-active resonance frequencies, ω_R, that coincide with the difference between two optical frequencies. This can yield a relatively straightforward source of coherent radiation, Raman-shifted at discrete intervals from the frequency ω_L of an input pump laser (either tunable or fixed wavelength). These Raman-shift intervals, both added to (anti-Stokes) and subtracted from (Stokes) the laser frequency ω_L, are integer multiples of ω_R. Other NLO Raman parametric processes give rise to various forms of nonlinear Raman spectroscopy, such as coherent anti-Stokes Raman scattering (CARS), and to Raman fiber-optical amplifiers, used in optical telecommunications. Another developing area of optical parametric device technology entails OPGs, OPAs, and OPOs based on $\chi^{(3)}$ nonlinearities in highly NLO fibers, with either pulsed or CW pump lasers. Such processes typically use two pump waves (P) to generate tunable signal (S) and idler (I) output waves, so that $\omega_I = 2\omega_P - \omega_S$.

2.2.2 $\chi^{(2)}$-Based Optical Parametric Gain and Amplification

The central theme of this chapter concerns $\chi^{(2)}$-based OPGs, OPAs, and OPOs, for which we can consider the intrinsic NLO process semiclassically in terms of three complex plane-wave radiation fields and the corresponding polarizations in the medium of interest:

$$\mathbf{E}_j(t) = \tfrac{1}{2}\mathbf{E}_j \exp\left[i\left(\mathbf{k}_j.\mathbf{r} - \omega_j t\right)\right] + \tfrac{1}{2}\mathbf{E}_j^{*}\exp\left[-i\left(\mathbf{k}_j.\mathbf{r} - \omega_j t\right)\right] \tag{2.6}$$

$$\mathbf{P}_j(t) = \tfrac{1}{2}\mathbf{P}_j \exp\left[i\left(\mathbf{k}_j.\mathbf{r} - \omega_j t\right)\right] + \tfrac{1}{2}\mathbf{P}_j^* \exp\left[-i\left(\mathbf{k}_j.\mathbf{r} - \omega_j t\right)\right] \tag{2.7}$$

where the suffix $j = $ P, S, or I. Interaction with the NLO susceptibility tensor $\boldsymbol{\chi}^{(2)}$ of a noncentrosymmetric medium then causes these to be interrelated as follows:

$$\mathbf{P}_S^{(2)} = \varepsilon_0 \boldsymbol{\chi}^{(2)} \mathbf{E}_P \mathbf{E}_I^*; \quad \mathbf{P}_I^{(2)} = \varepsilon_0 \boldsymbol{\chi}^{(2)} \mathbf{E}_P \mathbf{E}_S^*; \quad \mathbf{P}_P^{(2)} = \varepsilon_0 \boldsymbol{\chi}^{(2)} \mathbf{E}_S \mathbf{E}_I \tag{2.8}$$

where ε_0 is the vacuum permittivity (8.854×10^{-12} C^2/(J m)). Here, only the second-order polarizations $\mathbf{P}_j^{(2)}$ need be considered, and, in the interest of simplicity, the functional dependence of $\boldsymbol{\chi}^{(2)}$ on the optical frequencies ω_S, ω_I, ω_P has been suppressed.

It is significant that the polarizations $\mathbf{P}_j^{(2)}(t)$ for the coherent NLO processes, such as those represented in Equation 2.8, depend functionally on phase-dependent radiation fields $\mathbf{E}_j(t)$ as in Equation 2.6, rather than on phase-independent optical power or intensity. This phase dependence gives rise to phase-matching conditions—such as those in Equations 2.2, 2.3, and 2.5—in which the amplitude of $\mathbf{P}_j^{(2)}(t)$ is optimized (and hence the NLO output) when pump, signal, and idler waves are in phase for a maximum distance in the NLO medium.

Incidentally, use of the word *parametric* here is sometimes the cause of ambiguity. Parametric conversion processes were first recognized in the microwave context and were later carried over into the NLO domain. One highly regarded author suggests that all "elastic" NLO processes (in which initial and final material quantum states are identical and no real population is created elsewhere during the NLO process, which depends on a real susceptibility tensor $\boldsymbol{\chi}^{(2)}$) can be regarded as "parametric" [80]. This is in contrast to so-called nonparametric NLO processes, which are "inelastic" (with nonidentical initial and final material quantum states, and the photon energy is not conserved, because energy is transferred between the radiation field and the material); such nonparametric processes are independent of phase matching and depend on a complex susceptibility, for example, as in the $\boldsymbol{\chi}^{(1)}$ description of SRS [79,80]. All of the former "elastic" types of NLO process can, indeed, be treated by applying a parametric approximation, for example, to Equation 2.8, in the limit of low-strength signal and idler fields. However, the more widespread use [7–11,77–79] is for NLO parametric conversion to be a description that is confined to include processes such as those in OPGs, OPAs, and OPOs, but not those, for instance, in second harmonic, sum frequency, and DFGs (although these are "parametric processes" in the sense of [80]).

Continuing from Equations 2.6 through 2.8, we introduce a suitably defined, effective NLO coefficient d_{eff} (units: m V^{-1} or, more typically, pm V^{-1}) to yield [1,5]

$$P_S^{(2)} = 2\varepsilon_0 d_{eff} E_P E_I^*; \quad P_I^{(2)} = 2\varepsilon_0 d_{eff} E_P E_S^*; \quad P_P^{(2)} = 2\,\varepsilon_0 d_{eff} E_S E_I \tag{2.9}$$

where d_{eff} is a linear combination of elements of the NLO susceptibility tensor $\boldsymbol{\chi}^{(2)}$ for the medium of interest. For a particular BPM crystal, d_{eff} depends on its (noncentrosymmetric) crystal class and its cut and orientation relative to the propagation and

polarization directions of the incident light waves. The vector/tensor notation used in Equation 2.8 is not needed in Equation 2.9 for a specific experimental configuration.

By combining Equations 2.6, 2.7, and 2.9 with Maxwell's equations, our algebraic treatment of optical parametric amplification yields a set of relevant coupled wave equations for plane waves propagating in the z direction. These are common to various forms of three-wave NLO process, but are specified here for OPGs, OPAs, and OPOs [1,5]:

$$\left(\frac{dE_S}{dz}\right)+\alpha_S E_S = i\left(\frac{k_S}{{n_S}^2}\right) d_{\text{eff}} E_P E_I^* \exp\left(i\Delta k z\right) \tag{2.10}$$

$$\left(\frac{dE_I}{dz}\right)+\alpha_I E_I = i\left(\frac{k_I}{{n_I}^2}\right) d_{\text{eff}} E_P E_S^* \exp\left(i\Delta k z\right) \tag{2.11}$$

$$\left(\frac{dE_P}{dz}\right) = i\left(\frac{k_P}{{n_P}^2}\right) d_{\text{eff}} E_S E_I \exp\left(-i\Delta k z\right) \tag{2.12}$$

where α_j ($j = $ S, I, P) are loss factors and the wave-vector mismatch Δk is the z-component of $\Delta\mathbf{k}$.

Equation 2.12 corresponds to the customary limit of negligible pump-field losses ($\alpha_P = 0$). In addition, the pump wave may be treated as undepleted ($dE_P/dz = 0$) when it is much more intense than the other two waves, leaving only two coupled differential equations.

In parametric generation, the pump field, E_P, is assumed to be relatively strong, whereas the signal and idler fields, E_S and E_I, grow from a low level. In the zero-loss limit (with all $\alpha_j = 0$), Equations 2.10 through 2.12 yield what is effectively a photon conservation condition:

$$\omega_S^{-1}\left(\frac{dI_S}{dz}\right) = \omega_I^{-1}\left(\frac{dI_I}{dz}\right) = -\omega_P^{-1}\left(\frac{dI_P}{dz}\right);\ \ \lambda_S\left(\frac{dI_S}{dz}\right) = \lambda_I\left(\frac{dI_I}{dz}\right) = -\lambda_P\left(\frac{dI_P}{dz}\right) \tag{2.13}$$

where $I_j = \tfrac{1}{2}\, c\, \varepsilon_0\, n_j\, |E_j|^2$ (with $j = $ S, I, or P) is the optical intensity or flux (units: W m^{-1}). The conversion of each photon from the pump field (P) is then seen to generate two photons, one in the signal field (S) and the other in the idler field (I).

A situation that is more realistic than this zero-loss limit is that with finite but equal signal and idler losses ($\alpha_S = \alpha_I = \alpha$). This yields a tractable general solution describing the evolution of the signal and idler fields. In the case where a single-frequency idler field, $E_I(z)$, is incident on a pumped medium of length L, it experiences a single-pass power gain of the form:

$$G_I(L) = \left[\frac{|E_I(z=L)|^2}{|E_I(z=0)|^2}\right] - 1 = \Gamma^2 L^2 (gL)^{-2} \sinh^2(gL) \tag{2.14}$$